Journal of Nuclear Materials 390–391 (2009) 975–978

Contents lists available at ScienceDirect

Journal of Nuclear Materials

journal homepage: www.elsevier.com/locate/jnucmat

Investigation of chemical phase formation in the ternary system beryllium, carbon and tungsten with depth-resolved photoelectron spectroscopy

F. Kost *, Ch. Linsmeier, M. Oberkofler, M. Reinelt, M. Balden, A. Herrmann, S. Lindig

Max-Planck-Institut für Plasmaphysik, EURATOM Association, Boltzmannstrasse 2, 85748 Garching b. München, Germany

ARTICLE INFO

PACS:
52.40.Hf
82.80.Pv
41.60.Ap
82.40.−g

ABSTRACT

Synchrotron radiation XPS with different photon energies is used to gain depth-resolved chemical information. The temperature-dependent evolution of a ternary system sample with beryllium, carbon and tungsten is investigated. Five temperature steps are performed in order to analyze the kinetic processes and chemical states, namely 300, 530, 850, 1020 and 1200 K. After each temperature treatment, the sample composition is analyzed using four different information depths.

1. Introduction

For the future fusion experiment ITER, the three elements beryllium, carbon and tungsten are planned to be used as first wall materials [1]. The interaction between these materials, in particular the developing compounds due to temperature treatments, are of major interest as they strongly influence fusion-relevant material properties such as erosion behaviour, melting point and hydrogen inventory. The knowledge of binary systems is well established (e.g. [2]), but the complexity increases considerably with the addition of a third component. In order to understand these interactions, model systems with thin elemental layers of a few nm thicknesses are prepared, annealed and analyzed by X-ray photoelectron spectroscopy (XPS). For the characterization of temperature-driven processes such as diffusion, the XPS technique is applied using synchrotron radiation. By changing the excitation energy in the XPS process, it is possible to gain information from within different depths of the sample [3–7]. Compared to sputter depth profiling, this method has the advantage of being non-destructive and therefore does not alter the chemical composition of the investigated system. Hence, it allows an elemental and chemical state analysis as a function of depth.

2. Experimental

A carbon–beryllium–tungsten (C/Be/W) ternary system is prepared using physical vapour deposition. Polished polycrystalline tungsten is used as substrate material and carbon acts as a passivating layer on the top in order to minimise the influence of oxygen contaminations since it is less reactive towards oxidation than W and, particularly, Be. The beryllium layer is intermediate between the substrate and the carbon layer. The film thicknesses are 2.4 nm for the beryllium layer and 1.5 nm for the carbon layer. The sample is prepared under vacuum conditions (p < 8E-7 Pa during evaporation) and then transferred to the synchrotron beamline via transport through air.

XPS measurements are performed using a hemispherical electron analyzer at the MUSTANG endstation at the RGBL-PGM of the synchrotron facility BESSY in Berlin. The angle between the incident X-ray and the photoelectron take-off direction is 45°. For all the measurements, the photoelectron take-off direction is normal to the sample surface and the pass energy is 2 eV. The binding energy regions Be 1s, C 1s and W 4f are measured.

The sample is annealed at different temperatures and the XPS measurements are performed after cooling to 300 K after each temperature treatment of 530, 850, 1020 and 1200 K. The annealing time is 30 min for each step. In the photo-ionisation process, the photoelectron kinetic energy is determined by the incident photon excitation energy and the core level of the element emitting the photoelectrons (Be 1s, C 1s and W 4f in this work). As the kinetic energy of the photoelectrons strongly influences the inelastic mean free path [8], the excitation energy is chosen such that the photoelectrons originate from within the same depths, i.e. the inelastic mean free path is equal for different elements. Four different information depths are chosen for analysis.

For each spectrum, the binding energies are calibrated by measuring the Au 4f signal. Assuming a homogenous material, the intensity $I(E_k,x)$ for a photoelectron peak of kinetic energy E_k excited from the level x is given by $I(E_k,x) = J(h\nu)\ N_i\ \sigma(h\nu,\theta,x)\ \lambda(E_k)\ T(E_k)$, where $J(h\nu)$ is the photon flux incident on the sample at the energy $h\nu$, N_i is the density of atoms of the ith species, $\sigma(h\nu,\theta,x)$

* Corresponding author.
E-mail addresses: florian.kost@ipp.mpg.de (F. Kost), linsmeier@ipp.mpg.de (Ch. Linsmeier).

0022-3115/$ - see front matter © 2009 Elsevier B.V. All rights reserved.
doi:10.1016/j.jnucmat.2009.01.251

is the photoelectron cross section for the level x of the ith species at energy $h\nu$ and electron ejection angle θ; $\lambda(E_k)$ is the inelastic mean free path in the sample for electrons of kinetic energy E_k and $T(E_k)$ is the transmission function of the analyzer. The photon flux and the analyzer transmission are defined by the experimental setup. The photoelectron cross section $\sigma(h\nu,\theta,x)$ is separated into an angle-independent part and an angle-dependent asymmetry factor L, $\sigma(h\nu,\theta,x) = \sigma(h\nu,x)\cdot L(h\nu,\theta,x)$. For the polarized light used at the synchrotron beamline, the asymmetry factor is $L(h\nu,\theta,x) = 1 + 0.5\beta(3\cos^2\theta - 2)$, where β is the asymmetry parameter [9]. For quantitative analysis, the peak areas are normalized against photo-ionisation cross section [9], asymmetry parameter [10], ring current, photon flux and analyzer transmission.

Since one element is measured with different photon energies, the electrons have different inelastic mean free paths λ. Hence, taking into account the exponential attenuation of the intensity with depth, $I = I_0 \exp(-d/(\lambda \cos\theta))$, absolute peak areas from the same depths d are not comparable. Therefore, relative signal intensities are considered, which are normalized against the total signal intensity, which is the sum over all contributions. As the exact information depths for the photoelectrons cannot be determined, it is necessary to refer to the different depths as $d1$ (near-surface region) to $d4$ (largest information depth). Taking into account the mean free path dependence on photon energy, the chosen photoelectron kinetic energies are 60 eV (near-surface region), 300, 480 and 700 eV (largest information depth). Since relative signal intensities are normalized against the sum over all contributions, it is possible to compare relative signal intensities of different depth regions (even though the inelastic mean free path changes from $d1$ to $d4$).

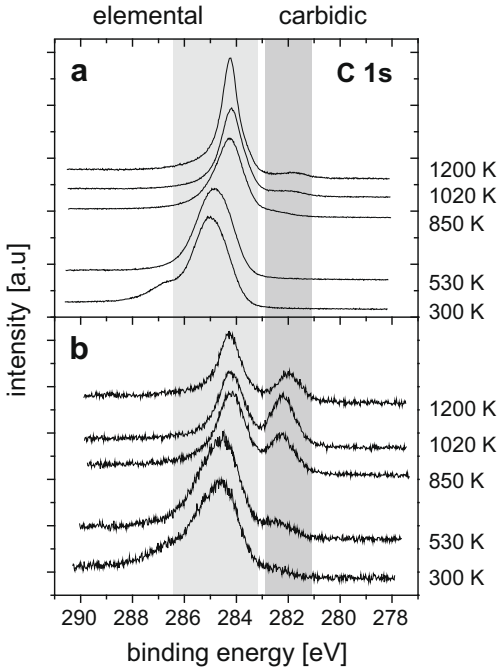

Fig. 1. XPS C 1s signal for 1.5 nm carbon and 2.4 nm beryllium layers evaporated on a tungsten substrate. The temperature steps are indicated on the right. The upper panel (a) shows measurements with a photoelectron kinetic energy of 60 eV (near-surface region, $d1$), while the lower panel shows data with a kinetic energy of 700 eV (largest information depth. $d4$). The beryllium carbide peak is developing at ~282 eV and expanding from the interface to the surface.

3. Results and discussions

Fig. 1 shows the C 1s signal after application of the previously described data treatments. Fig. 1(a) shows spectra in the C1s binding energy region with a photoelectron kinetic energy of 60 eV, while the measurements with a kinetic energy of 700 eV are shown in Fig. 1(b). The C 1s peak shape is fitted by background subtraction (Shirley background [11]) and three Gauss–Lorentz peaks: elemental carbon is described by a graphitic (E_B = 284.2 eV) and a disordered graphitic (E_B = 285.1 eV) contribution. The beryllium carbide peak is clearly visible in the binding energy region around 282 eV.

In the near-surface region (a), the carbide signal is not observed up to 850 K. At 1020 K, a small amount of Be_2C is detected. For the greater information depth (b), a certain amount of beryllium carbide is observed at room temperature. The carbide intensity rises during the temperature treatment and is most pronounced at 1020 K. At the last temperature, 1200 K, the beryllium carbide peak slightly shifts to lower binding energies. This binding energy shift might be due to the growth of Be_2C clusters and following cluster size effect. The cluster size is known to have an important influence on the binding energy [12]. The slight shift in the binding energy and peak shoulders at ~287 eV of the 300 and 580 K elemental carbon peaks indicates a surface contamination due to transport through air. This contribution is taken into account during the fitting procedure, but disregarded in the sample composition analysis.

The room temperature measurements are chosen to demonstrate the analysis of XPS spectra with different photon energies. The region $d1$ (photoelectron kinetic energy 60 eV) shows BeO with a relative signal intensity of 22% and elemental carbon with 78%. After sample preparation, no beryllium is present on the surface. This points to a Be diffusion (driven by the chemical gradient) to the surface when oxygen was available due to the transport through air.

The next information depth $d2$ (photoelectron kinetic energy 300 eV) shows 2% of metallic beryllium, 16% of BeO and 82% of elemental carbon. We want to emphasize here that the increasing kinetic energy of the photoelectrons increases the *information depth*, thus *adding* information of a greater depth to the overall measured relative elemental composition. Taking into account the exponential attenuation of the photoelectron intensity, the contribution from surface components is less influential as the information depth increases. Regarding the decreasing relative intensity of BeO for $d2$ from 22% to 16%, there is less BeO present in deeper regions. Vice versa, more elemental carbon is detected compared to $d1$. The relative signal intensities for $d3$ (photoelectron kinetic energy 480 eV) are 12% metallic Be, 3% beryllium carbide (Be_2C), 23% BeO and 62% elemental C. As there is a distinct contribution from metallic beryllium, the information depth now clearly exceeds the carbon overlayer. Both the Be and the BeO amounts increase for $d3$. As the relative signal intensity of BeO increases in measurement $d3$ compared to $d2$, this points not only to BeO at the surface but also to BeO in the metallic Be layer (below carbon). A small amount of Be_2C is detected at this information depth. Hence, the carbide formation at room temperature starts at the Be/C interface. Be_2C formation at room temperature has been investigated earlier [13]. The relative signal intensities for $d4$ (photoelectron kinetic energy 700 eV) are 18% metallic Be, 4% Be_2C, 25% BeO, 50% elemental carbon, and 2% metallic tungsten. Since the relative intensities for the beryllium components increase, there is more Be, Be_2C and BeO visible in $d4$. As there is a contribution from tungsten for $d4$, this information depth exceeds both the beryllium and carbon overlayers. The relative signal intensity of tungsten is not significant regarding the total sample composition, but nevertheless, metallic tungsten and a Be_2 W alloy are present.

The first annealing temperature is 530 K. The C 1s signal is taken as an example in Fig. 2 to point out the sample composition development during temperature treatments. The relative signal

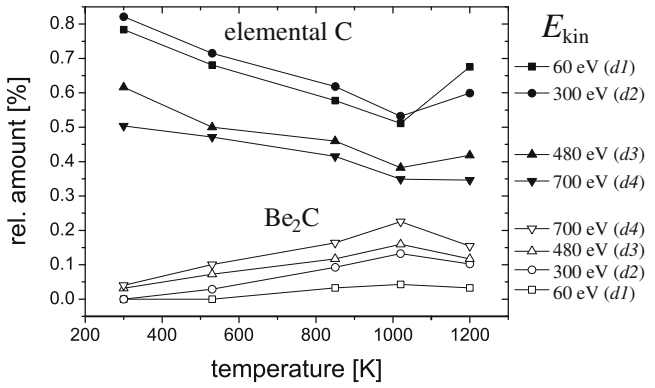

Fig. 2. Relative signal intensities of elemental carbon (solid symbols) and beryllium carbide (open symbols) as a function of temperature. The symbol shape indicates the photoelectron kinetic energy, as indicated on the right (*d*1 to *d*4 for near-surface and deepest analysis regions). The amount of beryllium carbide increases with increasing information depth. The change at 1200 K is due to a change in the surface morphology.

intensity of elemental carbon decreases from room temperature to the annealing step at 1020 K. The relative signal intensity is not maximal for *d*1, but for *d*2. This is due to the BeO overlayer, which is discussed above. As BeO is very prominent at the surface, the relative signal intensity of elemental carbon is smaller. Furthermore, the relative intensity of elemental carbon decreases from *d*2 to *d*4, since other contributions such as metallic Be and Be_2C become more prominent in greater depths. At the last temperature step, 1200 K, the relative signal intensity for elemental carbon is very prominent at the surface and decreases with increasing information depth. This might be due to carbon diffusion to the surface or a change in surface morphology, such as formation of island-like structures.

The relative signal intensity of Be_2C increases from *d*1 to *d*4. This indicates a beginning formation of beryllium carbide, starting at the Be/C interface and expanding to the surface. At the last temperature step, 1200 K, the overall relative signal intensity of Be_2C decreases. Since *relative* signal intensities are considered, the relative intensity of Be_2C is connected with that of elemental C.

At 530 K, the relative signal intensity of Be_2C increases for *d*3 and *d*4 and furthermore, Be_2C is detected in *d*2. This is another hint to beryllium carbide growth from the interface to the surface. According to an increasing Be_2C amount, the amounts of metallic Be and elemental carbon decrease. The amount of BeO at the surface is increasing due to rising pressure during temperature treatment, which gives rise to further oxide formation. Like for room temperature, a small contribution from tungsten is detected for *d*4 and the amount of the Be_2 W alloy is increasing.

At 850 K, the relative intensity of Be_2C increases for *d*2 to *d*4 and furthermore, Be_2C is detected in the near-surface region *d*1, giving another hint for carbide growth from the interface to the surface. The amount of BeO at the surface is increasing further and no metallic Be is left at this temperature step. As more Be_2C is forming, the total amount of elemental carbon decreases. At 850 K, the amount of Be_2 W is decreasing, whereas the onset of W_2C formation is observed.

At 1020 K, the relative intensity of Be_2C increases for *d*1 to *d*4. Furthermore, the amount of BeO at the surface increases. As no metallic Be is available to form additional Be_2C or BeO, this increase must be due to a change in surface morphology, thus giving more weight to near-surface components. According to the increase of Be_2C and BeO, the relative intensity of elemental carbon decreases for all depths. The relative signal intensity of tungsten is still not crucial regarding the total sample composition, but the amount of the Be_2 W alloy is further decreasing, whereas the amount of the subcarbide W_2C increases.

At 1200 K, the relative intensities of Be_2C and BeO decrease for *d*1 to *d*4, whereas the relative intensity of elemental carbon increases. As discussed for Fig. 2, this might be due to carbon diffusion to the surface or a change in surface morphology, such as formation of island-like structures. Furthermore, metallic tungsten and tungsten subcarbide W_2C is detected in the near-surface region *d*1. If tungsten diffusion was assumed, a carbide or alloy phase at the surface was expected. The presence of metallic tungsten can be ascribed to the appearing substrate which hints at the formation of island-like structures. At 1200 K, the Be_2 W alloy has completely vanished. The tungsten signal is composed of metallic and carbidic (W_2C) tungsten.

The results from the system Be/C/W are consistent with the analysis of binary systems. In experiments with carbon layers on a beryllium substrate, beryllium diffusion from the interface to the surface is observed [14]. At 770 K, Be_2C formation is complete [13]. Experiments with beryllium layers of a few nm thicknesses on a pyrolytic graphite substrate show island formation at 1070 K. In the ternary system, beginning formation of island-like structures is observed at 1020 K. Experiments with carbon layers on tungsten show C diffusion into the bulk material and W_2C formation starting at 870 K [15]. Alloy formation at room temperature is also observed in the binary system Be/W [16].

4. Summary

A layered system of beryllium, carbon and tungsten is prepared, annealed and analyzed by depth-resolved photoelectron spectroscopy. With this technique, it is feasible to characterize reactions by means of depth-resolved chemical information. Beryllium diffusion through carbon to the surface and BeO formation is observed at room temperature. The beryllium carbide formation starts at the interface and expands to the surface. It is complete at 850 K. Carbon diffuses into the bulk and starts forming W_2C at 850 K. At 1020 K, the analysis hints at a change in surface morphology. This effect is even more pronounced at 1200 K. The formation of a Be_2 W alloy is observed at room temperature. The alloy amount increases at 530 K; as the temperature rises to 850 K, the alloy amount is decreasing, whereas the amount of W_2C increases. The amount of tungsten carbide increases up to the last temperature 1200 K.

Acknowledgements

We thank Gianina Gavrialla, Maria Brzhezkinskaya and Mike Sperling for the support at the BESSY synchrotron beamline (RGBL-PGM).

References

[1] G. Federici, R. Anderl, J.N. Brooks, R. Causey, J.P. Coad, D. Cowgill, R. Doerner, A.A. Haasz, G. Longhurst, S. Luckhardt, D. Mueller, A. Peacock, M. Pick, C.H. Skinner, W. Wampler, K. Wilson, C. Wong, C. Wu, D. Youchison, Fus. Eng. Des. 39&40 (1998) 445.
[2] Ch. Linsmeier, AIP Conf. Proc. 740 (2004) 182.
[3] F. Esaka, K. Furuya, H. Shimada, M. Imamura, N. Matsubayashi, T. Sato, A. Nishijima, T. Kikuchi, A. Kawana, H. Ichimura, Surf. Sci. 377–379 (1997) 197.
[4] N. Matsubayashi, B.P. Singh, M. Imamura, T. Tanaka, Y. Sato, T. Ogiwara, M. Suzuki, S. Kiyota, Surf. Interface Anal. 36 (2004) 853.
[5] H. Shimada, N. Matsubayashi, M. Imamura, T. Sato, A. Nishijima, Appl. Surf. Sci. 100&101 (1996) 56.
[6] H. Shimada, K. Sato, N. Matsubayashi, M. Imamura, T. Saito, K. Furuya, Appl. Surf. Sci. 144&145 (1999) 21.
[7] M. Zier, S. Oswald, R. Reiche, K. Wetzig, Microchim. Acta 156 (2006) 99.
[8] M.P. Seah, W.A. Dench, Surf. Interface Anal. 1 (1979) 2.
[9] J.J. Yeh, I. Lindau, Atom. Data Nucl. Data 32 (1985) 1.
[10] M.P. Seah, I.S. Gilmore, Surf. Interface Anal. 31 (2001) 835.

[11] D.A. Shirley, Phys. Rev. B 5 (1972) 4709.
[12] M.G. Mason, Phys. Rev. B 27 (1983) 748.
[13] P. Goldstrass, K.U. Klages, Ch. Linsmeier, J. Nucl. Mater. 290–293 (2001) 76.
[14] J. Roth, W.R. Wampler, W.J. Jacob, J. Nucl. Mater. 250 (1997) 23.
[15] J. Luthin, Ch. Linsmeier, Surf. Sci. 454–456 (2000) 78.
[16] A. Wiltner, Ch. Linsmeier, J. Nucl. Mater. 337–339 (2005) 951.